Gene regulation mediated by calcium signals in T lymphocytes

Stefan Feske[1], Jena Giltnane[2], Ricardo Dolmetsch[3], Louis M. Staudt[2] and Anjana Rao[1]

Modulation of many signaling pathways in antigen-stimulated T and B cells results in global changes in gene expression. Here we investigate the contribution of calcium signaling to gene expression in T cells using cell lines from two severe-combined immunodeficiency patients with several cytokine deficiencies and diminished activation of the transcription factor NFAT nuclear factor of activated T cells. These T cells show a strong defect in transmembrane calcium influx that is also apparent in their B cells and fibroblasts. DNA microarray analysis of calcium entry–deficient and control T cells shows that Ca^{2+} signals both activate and repress gene expression and are largely transduced through the phosphatase calcineurin. We demonstrate an elaborate network of signaling pathways downstream of the T cell receptor, explaining the complexity of changes in gene expression during T cell activation.

Calcium plays an essential role in lymphocyte activation and maturation. Cross-linking of antigen or Fc receptors on T cells, B cells, mast cells and natural killer cells results in rapid increases in intracellular free calcium concentrations $[Ca^{2+}]$[1–4] and consequent activation of many transcription factors, including NFAT, NF-κB, JNK1, MEF2 and CREB[5]. In turn, these transcription factors regulate the expression of several inducible genes that mediate diverse genetic programs, including effector immune function, cell proliferation, cell differentiation and cell death[6].

Two stages of calcium mobilization have been distinguished in lymphocytes and other nonexcitable cells. The first stage involves activation of phospholipase Cγ by tyrosine kinases coupled to antigen and Fc receptors. This enzyme hydrolyzes phosphatidylinositol bisphosphate to release the second messenger inositol 1,4,5-trisphosphate (IP_3), which binds to its receptor in the endoplasmic reticulum (ER) membrane to cause rapid but transient release of Ca^{2+} from ER stores[7]. The second stage involves a sustained influx of extracellular Ca^{2+} across the plasma membrane, in a process termed "capacitative" or "store-operated" Ca^{2+} entry[8,9]. Capacitative calcium entry (CCE) occurs through specialized plasma membrane Ca^{2+} channels, which are notable in that depletion of intracellular Ca^{2+} stores suffices for their activation. Electrophysiologically, these depletion-activated channels—interchangeably termed store-operated Ca^{2+} channels (SOC) or calcium release–activated Ca^{2+} channels (CRAC)—show high selectivity for Ca^{2+}, very low single channel conductance and inward rectification[10]. However, their molecular identities and mode of activation remain controversial[11,12].

The two stages of calcium mobilization are differentially coupled to signaling pathways in T and B cells. The small transient spike of increased $[Ca^{2+}]_i$ elicited by store depletion is sufficient to activate certain signaling pathways and transcription factors such as NF-κB and JNK[5]. However, these brief calcium stimuli are insufficient for activation of other transcription factors, notably NFAT. NFAT normally resides in the cytoplasm of resting cells in a phosphorylated form; upon cellular stimulation it is dephosphorylated by the calcium-dependent phosphatase calcineurin, whereupon it translocates to the nucleus and shows increased transcriptional function[13–15]. NFAT activation is continuously regulated by the opposing actions of calcineurin and NFAT kinases, and both the nuclear translocation of NFAT and its activation of gene transcription are reversed by treatment of T cells with the calcineurin inhibitors cyclosporin A (CsA) and FK506[16,17]. As a result, sustained NFAT activation requires capacitative calcium entry and a sustained increase in $[Ca^{2+}]_i$[5,18,19].

We previously described two severe-combined immunodeficiency (SCID) patients with a principal defect in T cell activation and gene expression that was attributable to strongly impaired dephosphorylation and nuclear translocation of NFAT[20,21]. We show here that the impairment of NFAT activation in these patients is secondary to a pronounced defect in transmembrane calcium influx (CI). We used the patients' T cells as a tool to study calcium-dependent gene expression after stimulation. We show that Ca^{2+}-dependent signaling pathways mediate both gene induction and gene repression in activated T cells by integration of inputs from calcium store depletion, CI, calcineurin activation and other signaling pathways downstream of the T cell receptor (TCR).

Results

Increased $[Ca^{2+}]_{ex}$ compensates for NFAT defect

We previously showed that the defect in NFAT activation in the SCID patients' T cells could not be attributed to mutations or other functional defects, either in NFAT itself or in its regulating phosphatase calcineurin[21,22]. Therefore, we asked whether the defect in NFAT activation could be ameliorated in the presence of an increased concentration of extracellular Ca^{2+} ($[Ca^{2+}]_{ex}$). Control and patient T cells were stimulated with ionomycin in the presence of 0.8 or 2.8 mM $[Ca^{2+}]_{ex}$ for up to 2 h (**Fig. 1a**). In control T cells (**Fig. 1a**, left panels), complete and sustained dephosphorylation of NFAT1 (**Fig. 1a, A,B**), NFAT2 (**Fig. 1a, C,D**) and NFAT4 (data not shown) was observed at both $[Ca^{2+}]_{ex}$. In

[1]Center for Blood Research and Department of Pathology, [3]Children's Hospital, Harvard Medical School, Boston, MA 02115, USA. [2]Metabolism Branch, Division of Clinical Sciences, National Cancer Institute, Bethesda, MD 20892, USA. Correspondence should be addressed to A. R. (arao@cbr.med.harvard.edu).

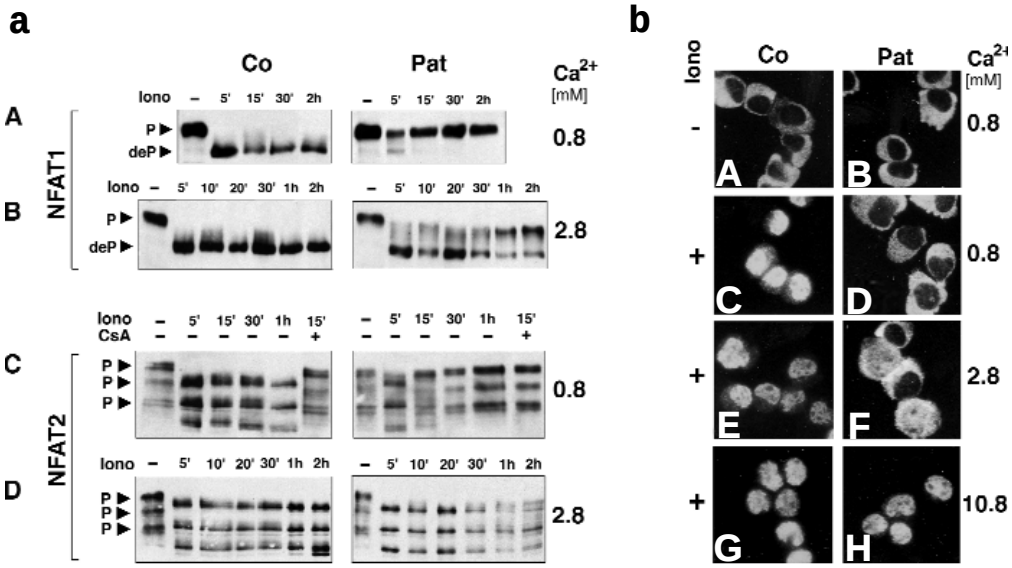

Figure 1. Dephosphorylation and nuclear translocation of NFAT in SCID patients' T cells is facilitated by high $[Ca^{2+}]_{ex}$. (**a**) Dephosphorylation: T cell lines established from one patient (Pat) and one control individual (Co) were left unstimulated or stimulated with ionomycin (Iono) in the presence of 0.8 mM (**A,C**) or 2.8 mM (**B,D**) $CaCl_2$. Where indicated, cells were preincubated with CsA before stimulation. Whole-cell extracts were prepared at the indicated time points and analyzed by immunoblotting. Arrows indicate the phosphorylated (P) and dephosphorylated (deP) forms of NFAT1 (**A,B**) and three phosphorylated splice variants of NFAT2 (**C,D**). Results are representative of several experiments with T cells from both patients and three independent controls. (**b**) Nuclear translocation: patient and control T cell lines were left unstimulated (**A,B**) or stimulated with ionomycin in the presence of 0.8 mM (**C,D**), 2.8 mM (**E,F**) or 10.8 mM (**G,H**) extracellular $CaCl_2$, and NFAT1 localization was assessed by immunocytochemistry.

contrast, in the patients' T cells (**Fig. 1a**, right panels), NFAT dephosphorylation was transient and incomplete at 0.8 mM $[Ca^{2+}]_{ex}$ but prolonged and almost complete at 2.8 mM $[Ca^{2+}]_{ex}$.

Similarly, NFAT nuclear translocation could be partially restored in the patients' T cells by increasing $[Ca^{2+}]_{ex}$. Before stimulation, NFAT1 was found in the cytoplasm in both control and patients' T cells (**Fig. 1b, A,B**). When cells were stimulated with ionomycin in the presence of 0.8 mM $[Ca^{2+}]_{ex}$, complete nuclear translocation was observed in control T cells (**Fig. 1b, C**), whereas NFAT1 in patients' T cells remained fully cytoplasmic (**Fig. 1b, D**). Increasing $[Ca^{2+}]_{ex}$ to 2.8 or 10.8 mM led to a graded increase in nuclear NFAT1 in the patients' T cells after ionomycin stimulation (**Fig. 1b, D,F,H**) without further effect in the control T cells (**Fig. 1b, C,E,G**). At 2.8 mM $[Ca^{2+}]_{ex}$, roughly 30% of the patients' T cells showed some amount of nuclear translocation, although most of the NFAT1 protein still resided in the cytoplasm (**Fig. 1b, F**), whereas at 10.8 mM $[Ca^{2+}]_{ex}$, about 80–90% of the patients' T cells showed complete nuclear translocation of NFAT1 (**Fig. 1b, H**). Elevation of $[Ca^{2+}]_{ex}$ to 10.8 mM also resulted in a low amount of cytokine gene transcription in the patients' T cells, especially for interleukin 5 (IL-5) and, to a lesser degree, also for IL-2, IL-4 and IFN-γ[22]. These results show that efficient expression of cytokine genes in T cells depends on complete and prolonged nuclear translocation of NFAT.

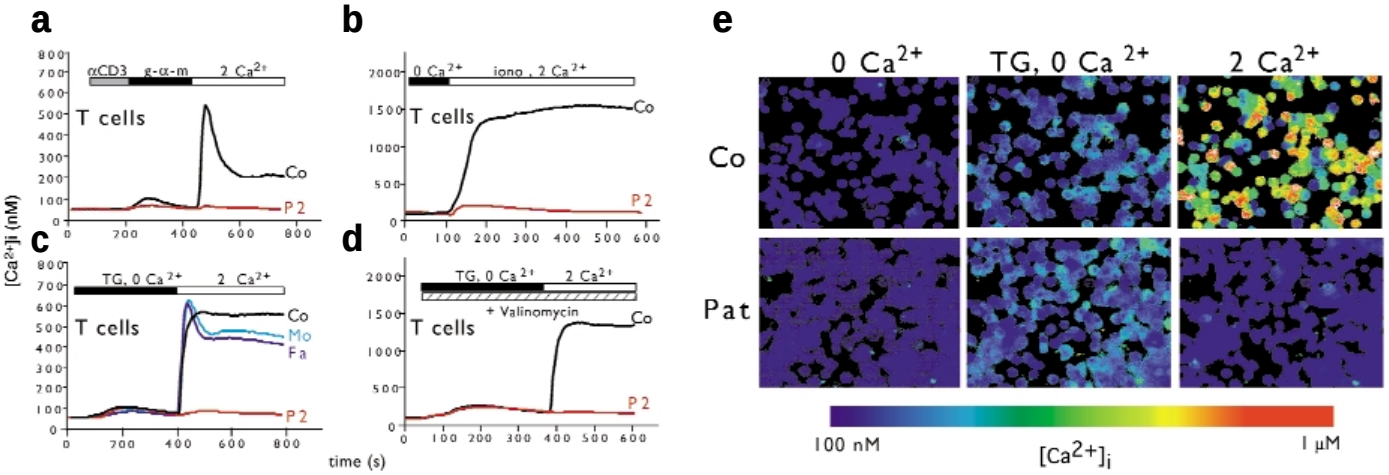

Figure 2. The SCID patients' T cells have a primary defect in transmembrane calcium influx. T cell lines established from one SCID patient (P2), the patient's mother (Mo) and father (Fa) and a normal control (Co) were loaded with Fura-2 and monitored for changes in intracellular free calcium. Data represent the means of >100–200 single cells. (**a**) For TCR-mediated cellular activation, T cells were incubated with anti-CD3 (α-CD3) in calcium-free Ringer solution, followed by cross-linking with goat anti–mouse IgG (g-α-m). Subsequently, cells were perfused with Ringer solution containing 2 mM $CaCl_2$ (2 Ca^{2+}). (**b**, **c**) For direct store depletion, T cells were stimulated either with (**b**) ionomycin (iono) in 2 Ca^{+} containing PMA or (**c**) thapsigargin (TG) in calcium-free Ringer solution (0 Ca^{2+}), followed by perfusion in 2 Ca^{2+}. (**d**) T cell lines were treated as in **c** but in the presence of valinomycin to hyperpolarize the cells. Each experiment is representative of several similar experiments conducted with both patients and two independent controls. (**e**) Comparison of microscopic single cell recordings of control (upper panels) and SCID patient's (lower panels) T cells (treated as in **c**). Digital images were taken immediately before addition of TG (left), 100 s after addition of TG (middle) and 5 min after addition of 2 Ca^{2+} (right). Graded color scale indicates Fura-2 emission ratios (340:380 nm), with purple representing low $[Ca^{2+}]_i$ and yellow/red representing high $[Ca^{2+}]_i$.

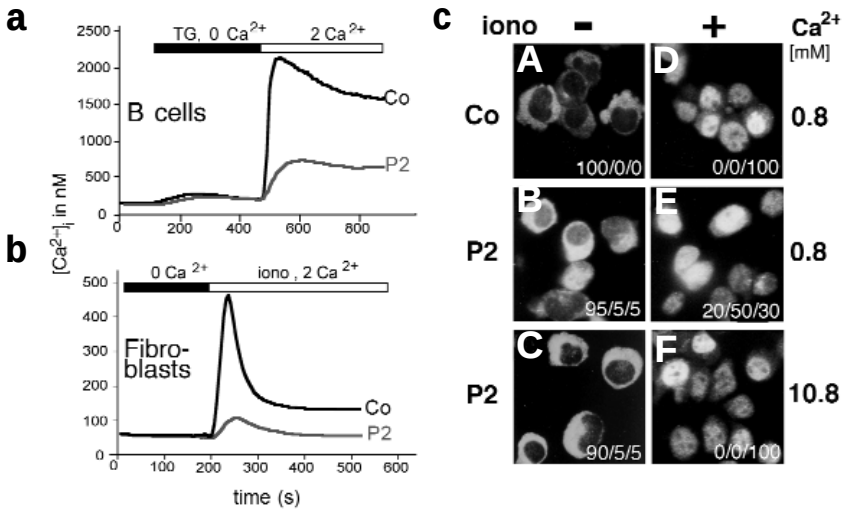

Figure 3. The calcium entry defect affects SCID patients' B cells and fibroblasts. EBV-transformed B cells (**a**) and untransformed fibroblasts (**b**) from patient 2 (P2) and a control (Co) were perfused with TG in calcium-free Ringer solution (0 Ca^{2+}), followed by Ringer solution containing 2 mM $CaCl_2$ (2 Ca^{2+}) alone. (**c**) EBV-transformed B cell lines from patient 2 and a control were left unstimulated or stimulated with ionomycin in the presence of the indicated $CaCl_2$ concentrations. Numbers in the panels refer to the approximate percentages of cells with cytoplasmic, partially nuclear and fully nuclear NFAT staining, respectively.

Calcium influx defect in SCID T cells

The strong dependence of NFAT activation on $[Ca^{2+}]_{ex}$ indicated a potential defect in calcium mobilization in the patients' cells. We used the Ca^{2+}-sensitive dye Fura-2 and compared stimulation-induced changes in $[Ca^{2+}]_i$ in single cells by digital video fluorescence imaging, mimicking TCR-dependent activation by cross-linking CD3 (**Fig. 2a**). In the absence of $[Ca^{2+}]_{ex}$, we observed a transient increase in intracellular calcium concentrations from ~50 nM to ~100 nM in control T cells that was attributable to depletion of intracellular calcium stores. Roughly 400 s after cross-linking, $[Ca^{2+}]_i$ reached resting concentrations again. Store depletion was also apparent in the SCID T cells, but to a lesser extent. Raising $[Ca^{2+}]_{ex}$ to 2 mM resulted in a steep increase in $[Ca^{2+}]_i$ in the control T cells (peak ~500 nM, with a sustained plateau at ~200 nM) that was not observed in the patient's T cells (**Fig. 2a**).

To determine whether the lack of $[Ca^{2+}]_i$ increase in the patient's T cells resulted from impaired TCR-mediated signaling leading to insufficient store depletion or inefficient activation of plasma membrane Ca^{2+} channels, we stimulated T cells with the calcium ionophore ionomycin (**Fig. 2b**). At low concentrations, this agent directly activates transmembrane CI by depleting internal Ca^{2+} stores[23]. Ionomycin stimulation of control T cells in the presence of 2 mM $[Ca^{2+}]_{ex}$ resulted in a steep increase in $[Ca^{2+}]_i$ from a resting concentration of ~80 nM to ~1.5 μM; $[Ca^{2+}]_i$ remained at this concentration for at least 30 min (**Fig. 2b** and data not shown). However, in the patient's T cells, the increase in $[Ca^{2+}]_i$ after ionomycin treatment was minimal (from a resting concentration of ~80 nM to ~200 nM at its peak 30 s after stimulation) and transient (returning to baseline ~300 s after stimulation initiation) (**Fig. 2b**). Thapsigargin, an inhibitor of the SERCA (sarcoplasmic endoplasmic reticulum calcium ATPase) which pumps calcium from the cytoplasm into the ER[24], was used to deplete internal Ca^{2+} stores independently of signals from surface receptors. We treated SCID and control T cells with thapsigargin in Ca^{2+}-free Ringer solution (**Fig. 2c,e**). Store depletion was observed as a transient rise in $[Ca^{2+}]_i$ in both SCID and control T cells. Increasing $[Ca^{2+}]_{ex}$ to 2 mM led to a steep increase of $[Ca^{2+}]_i$ in control T cells as well as in T cells from the patient's mother and father; in contrast, the patient's T cells showed an almost complete lack of $[Ca^{2+}]_i$ increase (**Fig. 2c,e**). Similar results were obtained with fluo-3 as calcium indicator in flow cytometry experiments (data not shown). Thus, defective coupling of store depletion to opening of plasma membrane Ca^{2+} channels is a likely explanation for the lack of Ca^{2+} mobilization in the SCID T cells.

Calcium influx through plasma membrane calcium channels is driven by the electrochemical gradient across the plasma membrane. To address the question of whether a reduced membrane potential in the SCID T cells accounted for the defect in Ca^{2+} influx, we assessed the membrane potential in patient and control T cells with a pair of voltage sensitive dyes, CC2-DMPE and $DiSBAC_2(3)$, which undergo changes in fluorescence resonance energy transfer when $DiSBAC_2(3)$ relocates from the outer to the inner leaflet of the plasma membrane as a result of alterations in membrane potential[25,26]. Untreated T cells from SCID patients and controls perfused in standard Ringer solution showed no systematic differences in resting membrane potential as judged by 460:570 nm emission ratios. In addition, both control and patient T cells showed comparable increases of the 460:570 ratio in response to stepwise depolarization with Ringer solution containing increasing KCl concentrations in place of NaCl (data not shown). Additionally, the calcium entry defect was not rescued by hyperpolarization of the patient's T cells with the potassium ionophore valinomycin (**Fig. 2d**). Although we have not yet fully ruled out the possibility of reduced driving force on calcium due to a membrane polarization defect, a primary defect in CCE seems more plausible based on the data discussed above. Formal proof of a CCE defect awaits patch-clamp measurements on the SCID T cells.

Calcium influx defect affects B cells and fibroblasts

To determine whether other cell types showed the defect in Ca^{2+} influx, we repeated the calcium imaging experiments with Epstein-Barr virus (EBV)-transformed B cell lines from SCID patient 2 and controls (**Fig. 3a**). Thapsigargin treatment of control and patient B cells in Ca^{2+}-free Ringer solution resulted in similar transient increases in $[Ca^{2+}]_i$. Upon addition of 2 mM $CaCl_2$, only the controls showed high intracellular calcium concentrations, with a plateau at ~1.5 μM $[Ca^{2+}]_i$; in contrast, the SCID B cells showed a much weaker response, with $[Ca^{2+}]_i$ ~600 nM. However, the defect was not as striking as that observed in the patient's T cells (compare with **Fig. 2c**). A similar impairment of Ca^{2+} influx was observed in nonimmune cells from SCID patients. Untransformed foreskin fibroblasts from one of the SCID patients and from a healthy donor were grown *in vitro* and stimulated with thapsigargin in Ca^{2+}-free Ringer solution. When perfused with 2 mM $CaCl_2$, controls showed a sharp spike of $[Ca^{2+}]_i$ to ~500 nM that lasted for ~150 s before reaching a plateau at ~150 nM $[Ca^{2+}]_i$. Conversely, the patient's fibroblasts showed a similarly transient, but much weaker, rise in $[Ca^{2+}]_i$, which peaked at ~100 nM and returned to baseline in ~4 min (**Fig. 3b**).

We investigated NFAT translocation in EBV-transformed B cell lines obtained from SCID patient 2 and healthy controls (**Fig. 3c**). As expected, NFAT1 was found in the cytoplasm in unstimulated control or patient B cells independent of $[Ca^{2+}]_{ex}$ (**Fig. 3c, A–C**). NFAT1

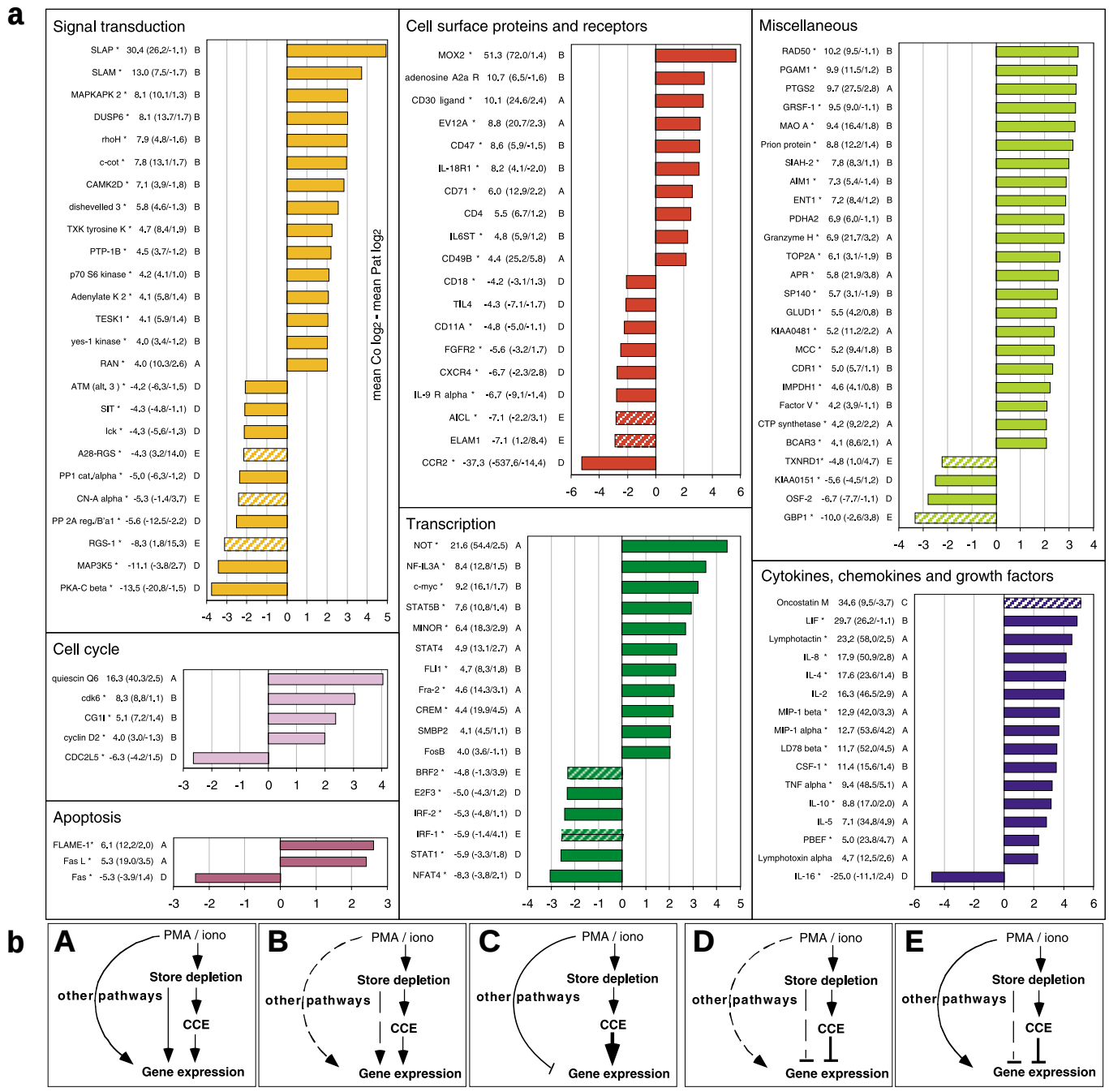

Figure 4. Calcium-dependent gene expression in T cells. (**a**) T cell lines of two patients and two normal controls were stimulated with PMA + ionomycin for 3 h and gene expression analyzed as described in Methods. Genes are grouped into broad functional groups. For each gene, the ratio of mRNA expression in stimulated *versus* unstimulated cells is listed in parentheses (control/patient), with positive and negative values indicating fold gene induction and repression, respectively. The ratio of these two values (induction/repression in control T cells divided by induction/repression in patient T cells) is given outside the parentheses and is plotted in the bar graphs on a base-2 logarithmic scale that indicates the degree to which gene induction is affected by the CI defect. A value of +2 indicates fourfold higher (that is, 400% of patient levels) induction of gene expression in control relative to patient T cells, whereas a value of -2 indicates fourfold lower (that is, 25% of control levels) induction in patients relative to controls. *Gene's identity was independently verified by sequencing of DNA clones. Genes were incorporated into this list if they showed at least threefold induction or repression in one of the two cell populations (patient or control) and at least a fourfold difference in induction or repression ratio in patient relative to control T cells. Capital letters behind the values for each gene refer to categories A–E in **b.** Cross-hatching is used to emphasize bars in categories C and E, which show opposing regulation by calcium *versus* other activation-induced signaling pathways. A more extensive list of genes can be found at http://lymphochip/nih.gov/SCID. (**b**) Categories A–E indicate different patterns of gene expression as described in the text and in the diagrams to the right.

translocation after ionomycin treatment at 0.8 mM $[Ca^{2+}]_{ex}$ was complete in control B cells (**Fig. 3c, D**), but remained incomplete in the SCID B cells (**Fig. 3c, E**). Under the same conditions, the patient's T cells showed no NFAT nuclear localization (**Fig. 1b, D**). When we increased $[Ca^{2+}]_{ex}$ to 10.8 mM, nuclear translocation of NFAT1 was complete as early as 15 min after stimulation in the control B cells but

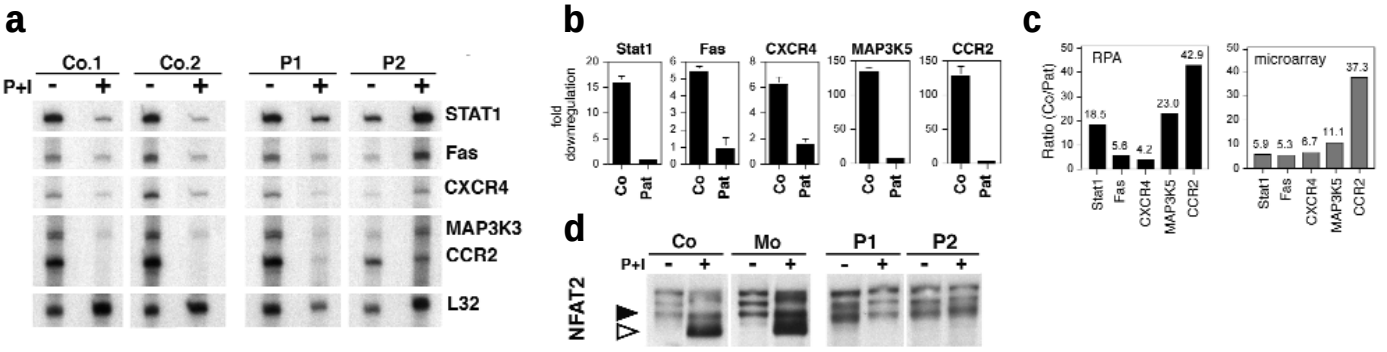

Figure 5. T cells deficient in calcium influx fail to repress the expression of certain genes. (**a**) RNase protection assays confirm down-regulation of five representative calcium-repressed genes. T cell lines from patients (P1, P2) and controls (Co1, Co2) were left unstimulated (–) or stimulated (+) with PMA + ionomycin and cytokine concentrations were assessed by RPA. (**b**) Fold down-regulation of the five genes from the RPA experiment shown in **a**. Transcript levels were quantified and normalized to expression of the housekeeping gene L32 after background subtraction and an average of the unstimulated:stimulated ratios from the two control and the two patient cell lines was taken. Error bars indicate range of duplicate values for two patients and two controls. The higher the value, the stronger the down-regulation of gene expression after stimulation. (**c**) Comparison of RPA and microarray data for the five genes shown in **a**. The ratios of fold decreases in gene expression in control and patients' T cells observed in RPA analyses (left) were compared with the same ratios obtained from the microarray experiments (right; and see number outside parentheses in Fig. 4). (**d**) Lack of induction of the CsA-sensitive NFAT2 splice variant[50] in the patients' T cells after prolonged stimulation. To confirm DNA array data showing that NFAT2 is induced in control T cells but not in patient T cells (see Fig. 6), T cells were stimulated with PMA + ionomycin (P+I) and NFAT2 was detected by immunoblotting using 7A6 mAb. Filled and open arrowheads indicate the phosphorylated and unphosphorylated forms of the short inducible NFAT2 isoform, respectively.

became complete only after 30 or 60 min in the patient's B cells (**Fig. 3c, F** and data not shown). Thus, unlike the patient's T cells, the patient's B cells show a clear, but partial, defect in NFAT activation. This is consistent with their partial defect in Ca^{2+} influx, which could result from a low residual function of the depletion-activated Ca^{2+} channels, from the activity of a related Ca^{2+}-specific channel or from Ca^{2+} leakage through nonselective cation channels at high $[Ca^{2+}]_{ex}$.

Ca^{2+} signals mediate gene activation and repression

Studying the contribution of Ca^{2+} signals to gene expression in T cells is difficult because truly specific inhibitors of CCE are not known. Therefore, we used the CI-deficient T cells to identify Ca^{2+} signaling–dependent genes using DNA microarrays, the preferred method for defining global patterns of gene expression, as it allows simultaneous assessment of the expression levels of thousands of messenger RNAs[6,27–29]. T cell lines of the two patients and two controls were left unstimulated or were stimulated with phorbol myristate acetate (PMA) + ionomycin for 3 h in RPMI medium in the presence of IL-2. cDNA derived from unstimulated and stimulated cells was labeled with Cy3 and Cy5, respectively, and incubated with specialized DNA "Lymphochip" microarrays containing genes relevant to lymphocyte function[30]. For each gene, we calculated the average fold increase in expression after stimulation for both control and patient T cell and plotted the ratio of these two induction values on a base-2 logarithmic scale (**Fig. 4a**). Genes were chosen whose expression was at least threefold increased (that is, 300% of baseline transcription) or decreased (33% of baseline transcription) as compared to resting expression in either the control or patient samples after stimulation, and also showed a fourfold or greater difference in expression between these two populations. Genes were then assigned to several groups according to their function. The list of genes is not comprehensive but is meant to illustrate the different patterns of gene expression; a more complete list can be found at http://lymphochip/nih.gov/SCID.

Of the 111 genes represented 79 (71%) were activated in response to sustained CI: they were induced to at least fourfold higher amounts in the control T cells than in the patients' CI-deficient T cells (**Fig. 4**, positive values). Forty-eight of these (61%) showed little or no change (less than twofold, that is, >50% and <200% of baseline transcription) in expression in the patients' T cells (**Fig. 4b**, category B); 30 (38%) were at least twofold (>200%) up-regulated in the patients' T cells after stimulation, although the degree of up-regulation was substantially less than that observed in the controls (**Fig. 4b**, category A); and one gene, oncostatin M, was 9.5-fold (950%) up-regulated in control T cells but 3.7-fold repressed (that is, 27% of baseline transcription) in patients' T cells after stimulation (**Fig. 4b**, category C, hatched bars). These different patterns indicate distinct underlying mechanisms for regulating gene expression (see later).

We found that 32 of the 111 genes (29%) showed evidence of calcium-mediated repression, which indicated at least fourfold stronger induction in CI-deficient than in control T cells (**Fig. 4b**, negative values for log base-2 induction ratio). Of these, 23 (72%) were expressed in basal amounts in resting T cells and were repressed by calcium signals after activation: their expression was strongly down-regulated in control T cells and unchanged or less strongly down-regulated in the patients' T cells (**Fig. 4b**, category D). This category includes the tyrosine kinase Lck; subunits of the serine and threonine phosphatases PP1 and PP2A; the transcription factors E2F-3, IRF-2 and STAT1; and the cell surface receptors Fas, CD18, CD11A and IL-9Rα. The remaining nine genes (28%) showed a converse behavior in that gene expression was actually induced in the patients' T cells, but either repressed, induced or induced to a significantly lesser extent (fourfold difference between patients and controls) in control T cells after stimulation (**Fig. 4b**, category E, hatched bars). A striking range of induction:repression ratios was observed in this category. For example, genes encoding the regulators of G-protein signaling A28-RGS and RGS-1 were 14- to 15-fold induced (1400–1500%) in the patients' T cells but only 2- to 3-fold induced (200–300%) in control T cells; thioredoxin reductase (TXNRD1) and IRF-1 were four- to fivefold (400–500%) up-regulated in the patients' T cells but unchanged in control T cells; CXCR4 was 2.8-fold up-regulated (280%) in the patients' T cells but 2.3-fold repressed (43%) in control T cells; and IL-16 (the only cytokine gene with this pattern of expression) was 2.4-fold up-regulated (240%) in the patients' T cells but 11-fold repressed (9%) in control T cells (**Fig. 4b**).

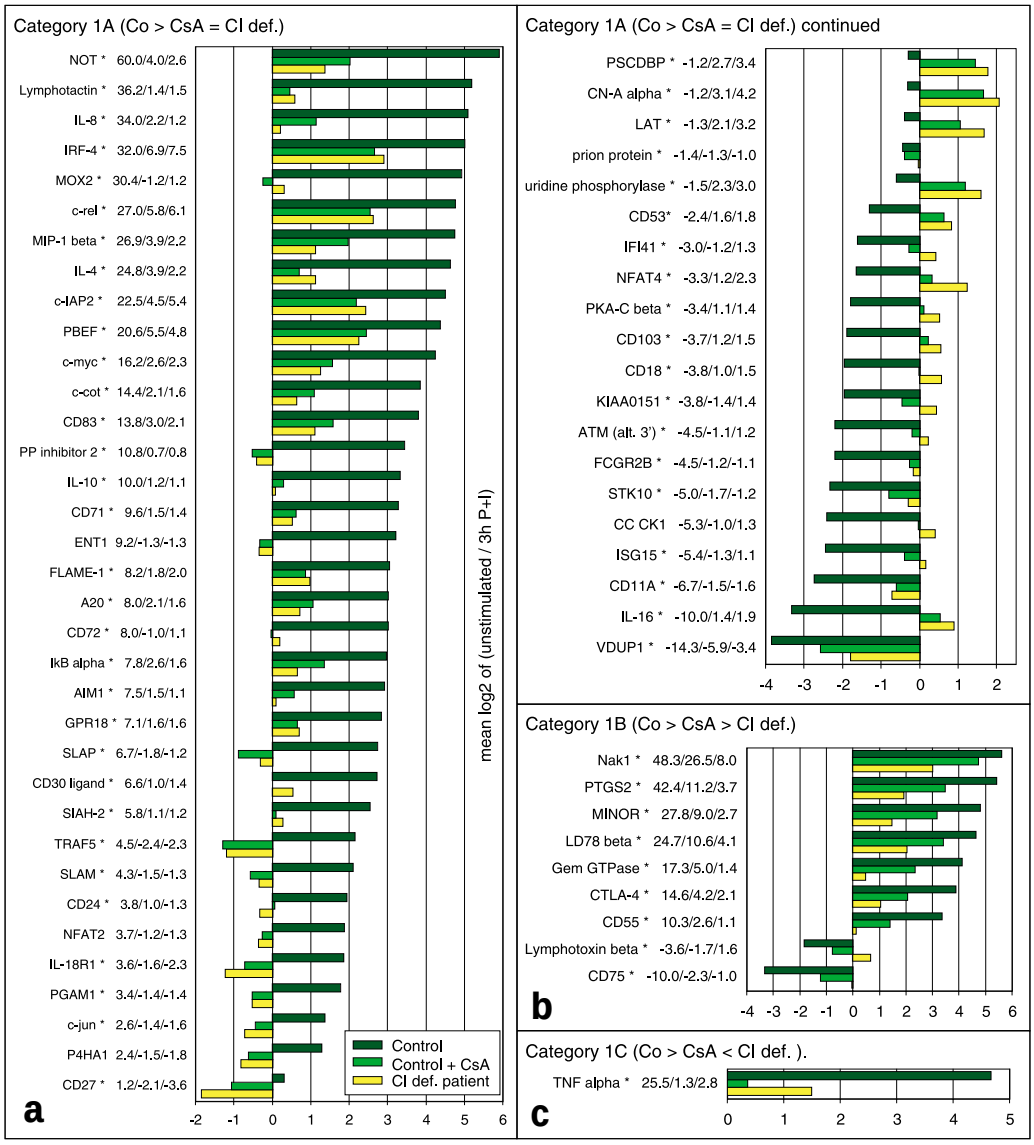

Figure 6. Calcineurin is involved in expression of most of calcium-regulated genes. Control and patient T cells were left unstimulated or stimulated with PMA + ionomycin for 3 h with or without preincubation with CsA. Bar sizes indicate ratios of gene expression in stimulated *versus* unstimulated cells for each gene; control T cells, dark green; CsA-treated control T cells, light green; patient T cells, yellow; positive values indicate fold induction; negative values indicate fold repression. Inclusion into this list required at least a fourfold difference in inducible gene expression in the control T cells or a fourfold difference between control and patient T cells. Categories refer to the dependence of gene expression on CI and calcineurin, as shown in Fig. 7. Category 1, CI-dependent genes (greater than twofold difference in induction:repression ratios between control, CsA-treated control and CI-deficient T cells). (**a**) Category 1A, calcium signal largely channeled through calcineurin (less than twofold difference between CsA-treated control and CI-deficient T cells). (**b**) Category 1B, calcineurin accounts for only a fraction of the calcium effect on gene expression (greater than twofold higher induction in CsA-treated control T cells compared with CI-deficient T cells). (**c**) Category 1C, TNF-α gene induction is more sensitive to CsA than to the CI defect (greater than twofold lower induction in CsA-treated control T cells compared with CI-deficient T cells). For other details see text and Fig. 4.

To confirm the calcium-mediated gene repression indicated by the DNA microarray analysis, we used the independent method of RNase protection assay (RPA) to assess the transcript levels of five genes that showed more abundant expression in the CI-deficient T cells (STAT1, Fas, CXCR4, MAP3K5 and CCR2; **Fig. 5a**). RNA was obtained from cells that were treated as for the microarray experiments (T cells of controls and patients were left unstimulated or stimulated with PMA + ionomycin for 3 h). Transcript levels were quantified and normalized to those of the housekeeping gene L32 and changes in expression levels were plotted as fold repression (**Fig. 5b**). In control T cells, expression of these five genes was strongly downregulated upon stimulation (~5 to ~130-fold), whereas in the CI-deficient T cells, transcript levels were effectively unchanged (**Fig. 5b**). The correlation between the RPA and microarray data was reasonably good, when comparing the ratio of inducible gene repression between patients and controls (**Fig. 5c**).

Ca^{2+}-mediated expression transduced by calcineurin

To determine the extent to which Ca^{2+} influx and calcineurin are required for the overall gene expression program in activated T cells, we conducted microarray analysis on cDNAs from control and CI-deficient patient T cells left unstimulated or stimulated with PMA + ionomycin (to assess CI-dependence), as well as from control T cells stimulated in the presence or absence of CsA (to assess calcineurin dependence). Genes were chosen for further study if they showed a fourfold or greater change in expression in either wild-type or patient T cells after stimulation or a fourfold difference between these two populations (**Fig. 6 & 7a**). Of 87 such induced or repressed genes, 22 (25%) were judged to be CI-independent, as they showed very similar induction or repression in control and CI-deficient T cells (**Fig. 7a**). In contrast, 65 of the 87 genes (75%) were judged to be CI-dependent, based on a fourfold or greater difference in degree of induction between wild-type and CI-deficient T cells (**Fig. 6**).

We used the data from this experiment to define CI-dependent genes that are regulated by calcineurin, other calcium-dependent pathways or both. CsA influenced, to a greater or lesser extent, induction of all 66 CI-dependent genes in category 1, which indicated that a principal function for calcineurin is transducing Ca^{2+} signals during T cell activation.

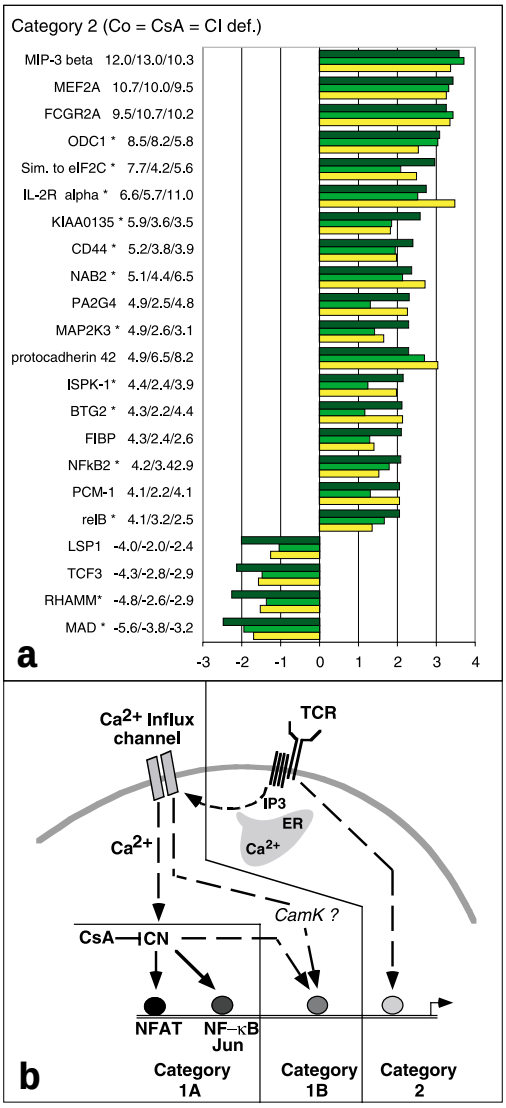

Figure 7. Calcineurin is involved in expression of most calcium-regulated genes. Control and patient T cells were treated as described and the data is displayed as in Fig. 6. (**a**) Category 2, CI-independent genes (less than twofold difference between control, CsA-treated control and CI-deficient T cells). For other details see text and Fig. 4. (**b**) Categories refer to the dependence of gene expression on CI and calcineurin. The scheme is drawn under the assumption that TCR stimulation is mimicked by PMA + ionomycin.

For ease of discussion, genes are subdivided into three relatively arbitrary categories. The largest subcategory, 1A (55/65 genes), contains genes that are strongly dependent on both CI and calcineurin, as their expression is as sensitive to calcineurin inhibition as to lack of CI. A much smaller subcategory, 1B (9/66 genes), contains genes for which calcineurin transduces only part of the Ca^{2+} signal: induction of these genes was less strongly suppressed by the calcineurin inhibitor CsA in control T cells than it was decreased in patient T cells that lack CI. A single gene (that which encoded TNF-α) is placed in subcategory 1C, based on the fact that it showed reproducibly higher induction in the patients' CI-deficient T cells than in CsA-treated control T cells. The basis for this behavior is not clear but may involve a component of induction through NF-κB. This transcription factor is CsA-sensitive in T cells, although its induction does not require sustained calcium influx, as it can be elicited by transient elevation of $[Ca^{2+}]_i$.

Discussion

We have shown that the primary defect in the SCID patients is a strong impairment of calcium mobilization in response either to TCR stimulation or exposure to the pharmacological agents ionomycin and thapsigargin. Stimulation of the patients' T cells through their TCRs failed to activate a sustained rise in intracellular free calcium concentrations; in addition, ionomycin and thapsigargin were unable to activate sustained Ca^{2+} influx, despite successful release of Ca^{2+} from the ER stores. We conclude that the defect is downstream of store depletion and does not involve kinases or adapter proteins known to couple TCR ligation to phospholipase C activation, IP_3 production and Ca^{2+} mobilization in T cells (for example, Lck, Itk, ZAP-70, LAT, SLP-76 and Vav, reviewed in[1]). However, it is noteworthy that the store depletion–related transient increase in $[Ca^{2+}]_i$ was lower in the patients' cells than in the control cells after CD3 cross-linking. The most likely explanation is an inability to replenish ER stores in the absence of transmembrane Ca^{2+} influx. However, a minor or secondary defect in TCR signaling cannot be entirely ruled out. The defect in the SCID T cells is also unlikely to be attributable to depolarization of the patients' cells relative to control cells: direct measurements of membrane potential with voltage-sensitive dyes did not show systematic differences between CI-deficient and control T cells. Also, deliberate hyperpolarization of the patients' T cells did not result in measurable reconstitution of CI. From these data, a primary defect in CCE is the most plausible explanation for the Ca^{2+} influx defect, although formal proof awaits patch-clamp measurements of the SCID T cells. Hence, it is likely that the mutation resides either in the depletion-activated calcium channels themselves or in a component of the general pathway that connects them to store depletion (reviewed in[10,12]).

The seven mammalian homologs of the *Drosophila* photoreceptor *TRP* (transient receptor potential) genes are candidate CRAC channel genes[32,33]. Similar to several other proteins, the IP_3 receptor, which is located in the ER membrane and interacts directly with mammalian TRP3[34–36], has been implicated in CRAC activation[12]. In addition, a similar clinical phenotype, with both a T cell activation defect and an impairment of transmembrane CI[37,38], has been described in another SCID patient. It would be useful to know whether these two immunodeficiencies and the Ca^{2+} influx–deficient Jurkat cells generated in other studies[39,40] fall into the same complementation group.

The defect in transmembrane Ca^{2+} influx is also observed in the patients' B cells and fibroblasts, and so may be responsible for functional deficits in diverse cell types and tissues. Indeed, the nonimmunological symptoms of the patients, which include nonprogressive muscular hypotonia and mild psychomotor and mental retardation[20,21], indicate a functional involvement of the mutated gene in muscle cells and neuronal cells. The defect is of lesser magnitude in B cells than in T cells, which is consistent with normal isotype switching and high to normal immunoglobulin production by the patients' B cells[31]. Potentially, B cells express both the mutant gene and a related gene, the product of which can compensate for the Ca^{2+} influx defect. Alternatively, EBV transformation may partially overcome the Ca^{2+} entry defect, either by induction of endogenous genes positively regulating calcium influx or because compensating proteins are encoded in the EBV genome.

Our results provide insight into the complex interplay between Ca^{2+}-dependent signaling pathways and other activation-induced signaling mechanisms in T cells. Only 25% of all activation-regulated genes

showed no dependence on Ca^{2+} influx. In the larger Ca^{2+}-dependent category, genes could be distinguished by whether they were positively or negatively regulated by calcium, the extent to which the calcium signals were transduced through calcineurin and the extent to which other (noncalcium-mediated) signaling pathways participate in their regulation.

Genes that were positively regulated by calcium fell into three categories, of which two (Categories A and B) are distinguished by their relative dependence on CI. Category A genes are discernibly up-regulated in CI-deficient patients' T cells, albeit to a lesser extent than in control T cells; thus, their expression must be mediated in part by CI and in part by other activation-induced signaling mechanisms. These mechanisms could be completely calcium-independent or could depend on transient $[Ca^{2+}]_i$ increases that do not involve CI. In contrast, category B genes are strongly dependent on CI: they are effectively silent in the patients' T cells, indicating an absolute requirement for $[Ca^{2+}]_i$ increases that are sustained for many hours. Genes in categories A and B are present in all functional groups, and include cytokine, chemokine and growth factor genes, cell surface receptors, transcription factors and signaling proteins known to be induced during a productive immune response. A third category (Category C) of positively regulated genes, represented by oncostatin M in our studies, is defined by up-regulation in control T cells but down-regulation in patients' T cells. This behavior points to a dual mode of regulation in which gene expression is activated by calcium but repressed by other signaling pathways emanating from the TCR.

Calcium-repressed genes (that is, genes that were up-regulated in patients' T cells relative to controls) were under-represented in the category of cytokine, chemokine and growth factor genes but were strongly represented in all other functional groups. Again, two different categories, D and E, could be distinguished. Category D genes show the converse behavior of categories A and B combined: store depletion and CI repress basal gene expression to greater or lesser extents in both control and patient T cells. Category E genes are the converse of category C: they are induced by noncalcium-dependent signaling pathways, and this induction is repressed by store depletion and/or CI. This behavior indicates a dual regulation whereby TCR signals other than calcium induce gene expression, although this induction is normally countered by CI-derived signals. Depending on the relative degree of TCR-mediated induction and calcium-mediated repression, a wide range of induction:repression ratios is possible and was, in fact, observed.

Whereas the mechanisms by which Ca^{2+} induces gene expression are well studied, less is known about how increases in $[Ca^{2+}]_i$ lead to gene repression. Calcium activates diverse transcription factors, including NFAT, NF-κB, Elk-1, Nur77, AP-1, ATF-2 and CREB, by calmodulin-dependent protein kinases and phosphatases[41–43]. Several mechanisms of Ca^{2+}-mediated gene activation have been described, many of which involve release of transcriptional repressor complexes from gene regulatory elements[44,45]. Particularly interesting are the diverse ways in which Ca^{2+} promotes dissociation of histone deacetylase complexes (HDAC) from the vicinity of the transcription factor MEF2D[46,47]. By analogy, it is conceivable that Ca^{2+} signals repress gene transcription by recruiting or activating HDACs or releasing or inhibiting histone acetyltransferases in an active transcriptional complex. In the absence of truly specific inhibitors of Ca^{2+} influx and CCE, T cells deficient in transmembrane CI will be valuable not only for potentially elucidating the mechanism of store-operated calcium entry but also for defining signaling pathways by which Ca^{2+} positively and negatively regulates gene expression.

Methods

Case report. Detailed case reports of the two SCID patients investigated in this study have been described[20,21].

Cell the culture conditions and reagents. Continuously growing T cell lines were derived from the peripheral blood lymphocytes (PBLs) of two patients before bone marrow transplantation, their parents and healthy donors, as described[20]. Cells were grown in the presence of 50 U/ml of recombinant human IL-2 (Hofmann LaRoche, Nutley, NJ). B cell lines were generated by isolation of $CD19^+$ cells from PBLs with dynabeads (Dynal, Lake Success, NY), transformed with EBV-containing supernatant derived from the marmoset cell line B95-8 and propagated in RPMI + 10% fetal bovine serum (FBS) (HyClone, Logan, UT) at 37 °C, 5% CO_2. Foreskin fibroblasts of the newborn Patient 2 were provided by C. Niemeyer; Hs27 control fibroblasts from a healthy newborn were from American Type Culture Collection (Manassas, VA). Cells were grown in RPMI 1640 + 10% FBS and split 1:4 every 4–5 days. For stimulation, $1–2\times10^6$ cells were treated with 1 μM ionomycin (Calbiochem, San Diego, CA) alone or in combination with 16.2 nM PMA (Calbiochem, La Jolla, CA) in RPMI + 10% FBS (containing a total estimated 0.8 mM $CaCl_2$). Where indicated, cells were preincubated for 15 min with 1 μM CsA (Calbiochem).

Immunoblotting and immunocytochemistry. Immunoblotting was done as described[21]. Antibodies used were anti-T2B1 to a COOH-terminal peptide of NFAT1c[48], mAb 7A6 to NFAT2 (Alexis Biochemicals, San Diego, CA), and a polyclonal antiserum to NFAT4 (gift of T. Hoey, Tularik Inc., South San Francisco, CA). Immunocytochemistry was done as described[21]. Where indicated, cells were stimulated with 1 μM ionomycin or 1 μM thapsigargin in RPMI + 10% FBS containing 0.8 mM $CaCl_2$. Anti-T2B1 for NFAT1 detection was used at 1:1000, followed by Cy-3–conjugated sheep anti-rabbit IgG (Sigma).

RNase protection assay. RNase protection assays were done according to manufacturers' protocol (Biotecx, Houston, TX), as described[21]. Briefly, cells were stimulated with 16.2 nM PMA and 1 μM ionomycin in RPMI + 10% FBS for 3 h and total cellular RNA was extracted with Ultraspec according to manufacturers' protocol. Cytokine RNA levels were analyzed by RNase protection assay using the RiboQuant multiprobe kits hck-3, hck-4 and a custom-made template set containing probes for STAT1, Fas, CXCR4, MAP3K5, CCR2 and L32 (PharMingen, San Diego, CA). Transcript levels were quantified by autoradiography and densitometric scanning of autoradiograms using a "Storm 860" phosphoimager and "imagequant" software (both Molecular Dynamics, Sunnyvale, CA). RNA loading was estimated by measuring the intensities of the protected fragments of the housekeeping gene L32.

Video imaging for calcium and voltage ratios. Cells were loaded at 1×10^6 cells/ml with 1 μM Fura-2 AM ester (Molecular Probes, Eugene, OR) in loading medium (RPMI + 10% FBS) for 30 min at room temperature, washed and resuspended in loading medium. Cells were attached to poly(L)lysine–coated coverslips for 15 min, mounted in a RC-20 closed bath flow chamber (Warner Instrument Corp., Hamden, CT) and analyzed on a TE-300 inverted epifluorescence microscope (Nikon, Melville, NY) with OpenLab imaging software (Improvision, Lexington, MA). Fibroblasts were grown directly on UV-treated sterile coverslips and loaded with fura-2. For recordings of cytoplasmic $[Ca^{2+}]_i$, cells were perfused in Ringer solution (155 mM NaCl, 4.5 mM KCl, 10 mM D-glucose, 5 mM Hepes at pH 7.4, 1 mM $MgCl_2$, 2 mM $CaCl_2$) and stimulated with either 1 μM ionomycin, 1 μM thapsigargin or 5 μg/ml of anti-CD3 (HIT 3A) cross-linked with 5 μg/ml of rat anti–mouse IgG2a (both from PharMingen). Where indicated, cells were first perfused in Ca^{2+}-free Ringer (in which Ca^{2+} was substituted by Mg^{2+}), followed by standard Ringer solution. Valinomycin was used at 1 μM where indicated. Fura-2 emission was detected at 510 nm after excitation of the dye at 340 and 380 nm, respectively, and ratios of 340:380 calculated for each 5-s interval after subtraction of background. Calibration values (R_{min}, R_{max}, S_f) were derived from cuvette measurements as described[49]. For each experiment, 100–200 cells were analyzed. For measurements of the membrane potential, 1×10^6 T cells were loaded with 1 μM coumarin lipid dye CC2-DMPE (Aurora Biosciences, San Diego, CA) for 30 min at room temperature in 1 ml of serum-free RPMI 1640 in the presence of 2 μl of 10% w/v Pluronic-127/DMSO solution (Aurora Biosciences). The oxonol dye $DiSBAC_2(3)$ (Aurora Biosciences) was loaded at 6 μM final concentration for 45 min at room temperature in RPMI 1640. Cells were loaded onto poly(L)lysine–coated coverslips and analyzed by video imaging at 405 nm (excitation) and 460 and 570 nm (emission), respectively. Depolarization was achieved by perfusing the cells in Ringer solution containing 20, 40, 60, 80, 100 and 155 mM KCl, respectively, with subsequent hyperpolarization using standard 4.5 mM KCl Ringer solution.

Messenger RNA samples and microarray procedures. T cell lines from healthy controls and the two SCID patients were left unstimulated or stimulated with 16.2 nM PMA and 1 μM ionomycin for 3 h with or without preincubation with 1 μM CsA for 15 min. For Fig. 6, T cell lines were enriched for $CD8^+$ cells to >90% purity using magnetic bead separation (Dynal, Lake Success, NY). Cells were collected at the indicated time points and poly(A) + mRNA isolated with the FastTrack Kit (Invitrogen, Carlsbad, CA). For each experiment, fluorescent cDNA probes were prepared by reverse transcription of mRNAs with Cy3-dUTP and Cy5-dUTP (NEN Life Sciences, Boston, MA) for unstimulated and stimulated samples, respectively. Labeled cDNAs were incubated overnight onto Lymphochip microarrays (L. Staudt, Bethesda, MD). Fluorescent images of hybridized microarrays were obtained using a GenePix 4000A microarray scanner (Axon Instruments, Foster City, CA).

Images were analyzed with GenePixPro3.0 (Axon Instruments) and single spots or areas of the array with obvious blemishes were flagged and excluded from subsequent analyses. Fluorescence ratios were stored in a custom database, and normalized data were extracted from this database for further analysis[28]. Array data were filtered by selecting genes that presented data on at least 75% of the arrays, had a spot diameter of ≥ 25 μm and a signal of ≥ 200 in each channel, or 1000 in one channel and some baseline signal in the other channel. In many cases, the given values in Figs. 4 and 6 are averages of several representations of one gene on the arrays. Genes are listed by their most commonly used names in the literature or, where ambiguous, based on HUGO-approved gene symbols. The cDNA clones on the Lymphochip microarray are available from Research Genetics. For Fig. 4, the samples were hybridized on Mini-Lymphochip version 4.0, which contained 7396 cDNA clones. Of these, 5335 (72.1%) passed the spot quality filters. For Fig. 6 the samples were hybridized on Mini-Lymphochip version 8.1, which contained 7392 cDNA clones, of which 3177 (42.9%) passed the spot quality filters. Genes included in our analysis were extracted from this pool. Results for genes with unclear function, uncharacterized genes and expressed sequence tags are not represented in Figs. 4 and 6 but will be available at http://lymphochip.nih.gov/SCID.

Acknowledgements

We thank C. Niemeyer for providing us with the patient data. Supported in part by grants from the Deutsche Forschungsgemeinschaft (Fe496/1-1) and in part by NIH grants CA42471 and AI40127.

Received 29 November 2000; accepted 12 February 2001.

1. van Leeuwen, J. E. & Samelson, L. E. T cell antigen-receptor signal transduction. *Curr. Opin. Immunol.* **11,** 242–248 (1999).
2. Braun, J., Sha'afi, R. I. & Unanue, E. R. Crosslinking by ligands to surface immunoglobulin triggers mobilization of intracellular 45Ca^{2+} in B lymphocytes. *J. Cell Biol.* **82,** 755–766 (1979).
3. Hoth, M. & Penner, R. Depletion of intracellular calcium stores activates a calcium current in mast cells. *Nature* **355,** 353–356 (1992).
4. Turner, H. & Kinet, J. P. Signalling through the high-affinity IgE receptor Fc epsilonRI. *Nature* **402,** 24–30 (1999).
5. Dolmetsch, R. E., Lewis, R. S., Goodnow, C. C. & Healy, J. I. Differential activation of transcription factors induced by Ca^{2+} response amplitude and duration. *Nature* **386,** 855–858 (1997).
6. Teague, T. K. *et al.* Activation changes the spectrum but not the diversity of genes expressed by T cells. *Proc. Natl Acad. Sci. USA* **96,** 12691–12696 (1999).
7. Berridge, M. J. Inositol trisphosphate and calcium signalling. *Nature* **361,** 315–325 (1993).
8. Putney, J. W., Jr. A model for receptor-regulated calcium entry. *Cell Calcium* **7,** 1–12 (1986).
9. Clapham, D. E. Intracellular calcium. Replenishing the stores. *Nature* **375,** 634–635 (1995).
10. Parekh, A. B. & Penner, R. Store depletion and calcium influx. *Physiol. Rev.* **77,** 901–930 (1997).
11. Putney, J. W. & Ribeiro, C. M. P. Signaling pathways between the plasma membrane and endoplasmic reticulum calcium stores. *Cell Mol. Life Sci.* **57,** 1272–1286 (2000).
12. Putney, J. W. "Kissin' cousins": intimate plasma membrane-ER interactions underlie capacitative calcium entry. *Cell* **99,** 5–8 (1999).
13. Okamura, H. & Rao, A. Transcriptional regulation in lymphocytes. *Curr. Opin. Cell. Biol.*, in press (2001).
14. Crabtree, G. R. Generic signals and specific outcomes: signaling through Ca^{2+}, calcineurin, and NF-AT. *Cell* **96,** 611–614 (1999).
15. Kiani, A., Rao, A. & Aramburu, J. Manipulating immune responses with immunosuppressive agents that target NFAT. *Immunity* **12,** 359–372 (2000).
16. Timmerman, L. A., Clipstone, N. A., Ho, S. N., Northrop, J. P. & Crabtree, G. R. Rapid shuttling of NF-AT in discrimination of Ca^{2+} signals and immunosuppression. *Nature* **383,** 837–840 (1996).
17. Loh, C. *et al.* Calcineurin binds the transcription factor NFAT1 and reversibly regulates its activity. *J. Biol. Chem.* **271,** 10884–10891 (1996).
18. Dolmetsch, R. E., Xu, K. & Lewis, R. S. Calcium oscillations increase the efficiency and specificity of gene expression. *Nature* **392,** 933–936 (1998).
19. Li, W., Llopis, J., Whitney, M., Zlokarnik, G. & Tsien, R. Y. Cell-permeant caged InsP3 ester shows that Ca^{2+} spike frequency can optimize gene expression. *Nature* **392,** 936–941 (1998).
20. Feske, S. *et al.* Severe combined immunodeficiency due to defective binding of the nuclear factor of activated T cells in T lymphocytes of two male siblings. *Eur. J. Immunol.* **26,** 2119–2126 (1996).
21. Feske, S., Draeger, R., Peter, H. H., Eichmann, K. & Rao, A. The duration of nuclear residence of NFAT determines the pattern of cytokine expression in human SCID T Cells. *J. Immunol.* **165,** 297–305 (2000).
22. Feske, S., Draeger, R., Peter, H. H. & Rao, A. Impaired NFAT regulation and its role in a severe combined immunodeficiency. *Immunobiology* **202,** 134–151 (2000).
23. Hofer, A. M., Fasolato, C. & Pozzan, T. Capacitative Ca^{2+} entry is closely linked to the filling state of internal Ca^{2+} stores: a study using simultaneous measurements of ICRAC and intraluminal [Ca^{2+}]. *J. Cell Biol.* **140,** 325–334 (1998).
24. Thastrup, O., Cullen, P. J., Drobak, B. K., Hanley, M. R. & Dawson, A. P. Thapsigargin, a tumor promoter, discharges intracellular Ca^{2+} stores by specific inhibition of the endoplasmic reticulum Ca2(+)-ATPase. *Proc. Natl Acad. Sci. USA* **87,** 2466–2470 (1990).
25. Gonzalez, J. E. & Tsien, R. Y. Improved indicators of cell membrane potential that use fluorescence resonance energy transfer. *Chem. Biol.* **4,** 269–277 (1997).
26. Gonzalez, J. E. & Tsien, R. Y. Voltage sensing by fluorescence resonance energy transfer in single cells. *Biophys. J.* **69,** 1272–1280 (1995).
27. DeRisi, J. L. & Iyer, V. R. Genomics and array technology. *Curr. Opin. Oncol.* **11,** 76–79 (1999).
28. Alizadeh, A. A. *et al.* Distinct types of diffuse large B-cell lymphoma identified by gene expression profiling. *Nature* **403,** 503–511 (2000).
29. Rogge, L. *et al.* Transcript imaging of the development of human T helper cells using oligonucleotide arrays. *Nature Genet.* **25,** 96–101 (2000).
30. Alizadeh, A. *et al.* The Lymphochip: a specialized cDNA microarray for the genomic-scale analysis of gene expression in normal and malignant lymphocytes. *Cold Spring Harb. Symp. Quant. Biol.* **64,** 71–78 (1999).
31. Schlesier, M. *et al.* Primary severe immunodeficiency due to impaired signal transduction in T cells. *Immunodeficiency* **4,** 133–136 (1993).
32. Montell, C. New light on Trp and Trpl. *Mol. Pharmacol.* **52,** 755–763 (1997).
33. Putney, J. W. & McKay, R. R. Capacitative calcium entry channels. *Bioessays* **21,** 38–46 (1999).
34. Ma, H. T. *et al.* Requirement of the inositol trisphosphate receptor for activation of store-operated Ca^{2+} channels. *Science* **287,** 1647–1651 (2000).
35. Boulay, C. *et al.* Modulation of Ca^{2+} entry by polypeptides of the inositol 1,4,5-trisphosphate receptor (IP3R) that bind transient receptor potential (TRP): evidence for roles of TRP and IP3R in store depletion-activated Ca^{2+} entry. *Proc. Natl Acad. Sci. USA* **96,** 14955–14960 (1999).
36. Kiselyov, K., Mignery, G. A., Zhu, M. X. & Muallem, S. The N-terminal domain of the IP3 receptor gates store-operated hTrp3 channels. *Mol. Cell* **4,** 423–429 (1999).
37. Partiseti, M. *et al.* The calcium current activated by T cell receptor and store depletion in human lymphocytes is absent in a primary immunodeficiency. *J. Biol. Chem.* **269,** 32327–32335 (1994).
38. Le Deist, F. *et al.* A primary T-cell immunodeficiency associated with defective transmembrane calcium influx. *Blood* **85,** 1053–1062 (1995).
39. Fanger, C. M., Hoth, M., Crabtree, G. R. & Lewis, R. S. Characterization of T cell mutants with defects in capacitative calcium entry. Genetic evidence for the physiological roles of crac channels. *J. Cell Biol.* **131,** 655–667 (1995).
40. Serafini, A. T. *et al.* Isolation of mutant T lymphocytes with defects in capacitative calcium entry. *Immunity* **3,** 239–250 (1995).
41. Rao, A., Luo, C. & Hogan, P. G. Transcription factors of the NFAT family: regulation and function. *Annu. Rev. Immunol.* **15,** 707–747 (1997).
42. Aramburu, J., Rao, A. & Klee, C. B. Calcineurin: from structure to function. *Curr. Top. Cell Regul.* **36,** 237–295 (2000).
43. Tokumitsu, H., Enslen, H. & Soderling, T. R. Characterization of a Ca^{2+}/calmodulin-dependent protein kinase cascade. Molecular cloning and expression of calcium/calmodulin-dependent protein kinase kinase. *J. Biol. Chem.* **270,** 19320–19324 (1995).
44. Carrion, A. M., Link, W. A., Ledo, F., Mellstrom, B. & Naranjo, J. R. DREAM is a Ca^{2+}-regulated transcriptional repressor. *Nature* **398,** 80–84 (1999).
45. McKinsey, T. A., Zhang, C. L., Lu, J. R. & Olson, E. N. Signal-dependent nuclear export of a histone deacetylase regulates muscle differentiation. *Nature* **408,** 106–111 (2000).
46. Youn, H. D., Grozinger, C. M. & Liu, J. O. Calcium regulates transcriptional repression of myocyte enhancer factor 2 by histone deacetylase 4. *J. Biol. Chem.* **275,** 22563–22567 (2000).
47. Youn, H. D., Sun, L., Prywes, R. & Liu, J. O. Apoptosis of T cells mediated by Ca^{2+}-induced release of the transcription factor MEF2. *Science* **286,** 790–793 (1999).
48. Wang, D. Z., McCaffrey, P. G. & Rao, A. The cyclosporin-sensitive transcription factor NFATp is expressed in several classes of cells in the immune system. *Ann. NY Acad. Sci.* **766,** 182–194 (1995).
49. Grynkiewicz, G., Poenie, M. & Tsien, R. Y. A new generation of Ca^{2+} indicators with greatly improved fluorescence properties. *J. Biol. Chem.* **260,** 3440–3450 (1985).
50. Chuvpilo, S. *et al.* Alternative polyadenylation events contribute to the induction of NF- ATc in effector T cells. *Immunity* **10,** 261–269 (1999).